Article

SOURCE DATA | TRANSPARENT PROCESS

THE EMBO JOURNAL

Meiotic cohesin STAG3 is required for chromosome axis formation and sister chromatid cohesion

Tristan Winters, Francois McNicoll & Rolf Jessberger*

Abstract

The cohesin complex is essential for mitosis and meiosis. The specific meiotic roles of individual cohesin proteins are incompletely understood. We report *in vivo* functions of the only meiosis-specific STAG component of cohesin, STAG3. Newly generated STAG3-deficient mice of both sexes are sterile with meiotic arrest. In these mice, meiotic chromosome architecture is severely disrupted as no *bona fide* axial elements (AE) form and homologous chromosomes do not synapse. Axial element protein SYCP3 forms dot-like structures, many partially overlapping with centromeres. Asynapsis marker HORMAD1 is diffusely distributed throughout the chromatin, and SYCP1, which normally marks synapsed axes, is largely absent. Centromeric and telomeric sister chromatid cohesion are impaired. Centromere and telomere clustering occurs in the absence of STAG3, and telomere structure is not severely affected. Other cohesin proteins are present, localize throughout the STAG3-devoid chromatin, and form complexes with cohesin SMC1β. No other deficiency in a single meiosis-specific cohesin causes a phenotype as drastic as STAG3 deficiency. STAG3 emerges as the key STAG cohesin involved in major functions of meiotic cohesin.

Keywords chromosomes; cohesin; meiosis; oocytes; spermatocytes
Subject Categories Cell Cycle
DOI 10.1002/embj.201387330 | Received 5 November 2013 | Revised 8 April 2014 | Accepted 9 April 2014 | Published online 5 May 2014
The EMBO Journal (2014) 33: 1256–1270

See also: **T Fukuda *et al*** (June 2014)

Introduction

Cohesin is essential for sister chromatid cohesion and contributes to DNA repair and recombination, to the regulation of gene expression and chromosome architecture (for reviews, see Haering & Jessberger, 2012; Nasmyth, 2011; Nasmyth & Haering, 2009; Onn *et al*, 2008; Shintomi & Hirano, 2010; Wood *et al*, 2010). The tripartite core cohesin complex consists of the SMC1 and SMC3 (structural maintenance of chromosome) proteins and a kleisin protein which closes the somewhat V-shaped SMC1/3 heterodimer to a ring-like complex. Cohesin associates through its kleisin subunit with a fourth protein called STAG or SA (stromalin) in vertebrates, initially identified in human and *Xenopus laevis* cohesin complexes (Losada *et al*, 2000; Sumara *et al*, 2000), and named Scc3p in *Saccharomyces cerevisiae* (Michaelis *et al*, 1997). Despite very important recent progress, the functions of STAG proteins are still the least understood of any of the cohesin proteins. In vertebrates, there are three STAG/SA variants called STAG or SA1 to SA3, and the cohesin complex associates with one of them.

SA1 and SA2 are ubiquitously expressed and appear to serve as interaction platforms of cohesin with other factors. For example, the insulator protein CTCF, which functionally interacts with and depends on cohesin, associates with SA2 (Xiao *et al*, 2011), which was also reported to interact with transactivator proteins (Lara-Pezzi *et al*, 2004). SA1 also regulates transcription and cohesin binding to genomic sites also bound by CTCF (Remeseiro *et al*, 2012b). In addition, SA1 is required for sister chromatid cohesion at telomeres, while SA2 is necessary for centromeric cohesion (Canudas & Smith, 2009). In mice, heterozygous SA1 deficiency increases tumorigenesis, and embryonic fibroblasts derived from homozygous $Sa1^{-/-}$ mice show telomere-associated chromosome segregation defects and increased aneuploidy (Remeseiro *et al*, 2012a). SA1 is enriched at telomeres in HeLa cells and directly binds telomeric DNA through a characteristic motif, an AT hook (Bisht *et al*, 2013). Phosphorylation of STAG proteins was reported in meiotic cells (Fukuda *et al*, 2012), and in mitotic cells, SA2 phosphorylation is required for dissolution of sister chromatid arm cohesion in prophase and prometaphase (Hauf *et al*, 2005). Potential roles of cohesins including STAG proteins in human cancer, whether tumor-promoting or tumor-suppressing depending on the circumstances such as overexpression, mutation, or protein loss, are currently debated (Solomon *et al*, 2011; Balbas-Martinez *et al*, 2013).

STAG3 was initially shown to be specific to spermatocytes where it associates with the meiosis-specific synaptonemal complex (SC; Pezzi *et al*, 2000). In early prophase I of meiosis, each pair of sister chromatids forms a structure called the axial element (AE). The AEs of homologous chromosomes start to pair and synapse in zygonema and in pachynema have completed synapsis into the SC, where the AEs are termed lateral elements (LEs). The SC is a ladder-like protein-DNA structure and consists of several meiosis-specific proteins including SYCP2 and SYCP3, present in the LEs of the 'ladder', the transverse filament protein SYCP1, and several central

Medical Faculty Carl Gustav Carus, Institute of Physiological Chemistry, Technische Universität Dresden, Dresden, Germany
*Corresponding author. Tel: +49 351 458 6446; Fax: +49 351 458 6305; E-mail: rolf.jessberger@tu-dresden.de

element proteins. While SYCP2 and 3 associate with the axes in leptonema when the AEs form, SYCP1 associates only upon synapsis. STAG3 was found to be associated with AEs and LEs and accumulates at the intersister chromatid domain, consistent with its potential role in sister chromatid cohesion (Prieto *et al*, 2001). STAG3 also associates with the paired and unpaired regions of the X and Y sex chromosomes and partially co-localizes with the inner centromeres and is also found at telomeres (Liebe *et al*, 2004). With progression of meiosis beyond pachynema, that is, with dissolution of the SC, STAG3 dissociates from the chromosome axes. At the metaphase to anaphase I transition, STAG3 disappears from chromosome arms and remains chromosome-associated at the centromeres. In anaphase I, STAG3 vanishes entirely and is not observed at later stages of meiosis. In other vertebrates such as marsupials, a similar localization of STAG3 in spermatocytes was reported (Page *et al*, 2006) and expression patterns in human testis, ovary, spermatocytes, and oocytes are consistent with the observations in mice and a role in sister chromatid cohesion (Houmard *et al*, 2009; Nogues *et al*, 2009; Garcia-Cruz *et al*, 2010). In oocytes, a similar pattern of chromosome associations was observed where STAG3 is found along chromosome axes from leptonema to diplonema and dissociates during dictyate arrest (Prieto *et al*, 2004). In aged oocytes from senescence-accelerated mice, STAG3 levels, like those of other cohesin proteins, are significantly reduced (Liu & Keefe, 2008), consistent with the hypothesis of the loss of cohesin as a major contributor to increased age-dependent aneuploidy (reviewed in Jessberger, 2010, 2012). Very recently, a 1-bp deletion in the *Stag3* gene that causes a frameshift was found in patients of a family affected by premature ovarian failure. If translated and stable, this would lead to a small truncated protein of 194 amino acids of 1,225 amino acids (Caburet *et al*, 2014).

Besides STAG3, the SA1 and SA2 (Prieto *et al*, 2002) proteins are also present in early prophase I, but their biological functions in meiocytes are unclear. Mammalian meiocytes express three additional meiosis-specific cohesin proteins: one SMC1 protein variant called SMC1β and two kleisins, REC8 and RAD21L. Together with the ubiquitous SMC1α, SMC3, and the kleisin RAD21, multiple combinations of cohesin proteins form several distinct complexes in meiocytes. Cohesin serves several functions in meiosis. Perhaps most prominently, cohesin determines meiotic chromosome architecture. Removal of individual cohesin proteins such as SMC1β or REC8 causes shortening of prophase I chromosomal axes (Bannister *et al*, 2004; Revenkova *et al*, 2004; Xu *et al*, 2005; Herran *et al*, 2011). The simultaneous elimination of both meiosis-specific kleisins, REC8 and RAD21L, largely abolishes axis formation (Llano *et al*, 2012).

Here, we report on the role *in vivo* of the only meiosis-specific STAG protein, STAG3. It remained unclear whether STAG3 is essential for meiosis and whether it acts in one or several of the meiotic processes mentioned above. Further, it was unknown whether STAG3-associated cohesin complexes represent a major functional fraction of the cohesin complexes in mammalian meiocytes. Therefore, we set out to investigate the role of STAG3 using a STAG3-deficient mouse strain and revealed an essential function of STAG3 in meiosis. STAG3-deficient spermatocytes and oocytes suffer from an absence of chromosome axes and impaired sister chromatid cohesion and are eliminated during meiosis. Thus, STAG3, which is present in the most prominent types of cohesin complexes in mammalian meiocytes, represents the key STAG protein acting in major functions of meiotic cohesin.

Results

Infertility of STAG3-deficient mice

The embryonic stem cell *Stag3*$^{tm1a(KOMP)Wtsi}$ was obtained from KOMP and injected into blastocysts to produce the respective *Stag3* mutant strain. This strain carries a knockout-first cassette, designed to block gene expression after its insertion through providing a splice acceptor in the lacZ component of the insert, from which no further splicing occurs (Supplementary Fig S1).

We bred this strain to homozygosity (named *Stag3*$^{ko/ko}$ to indicate its 'knockout-first' design). Male and female *Stag3*$^{ko/ko}$ were infertile but otherwise healthy. The testes of *Stag3*$^{ko/ko}$ mice were less than half the size and weight of those of wild-type (wt) mice (Fig 1A). The presence of *Stag3* mRNA was assessed by RT-PCR diagnostic for transcription and/or splicing across or flanking the knockout-first insertion (Supplementary Fig S1). This confirmed the disruption of *Stag3* gene expression (Fig 1B). STAG3 protein was also absent in *Stag3*$^{ko/ko}$ testis nuclear extracts analyzed by immunoblotting (IB; Fig 1C). In testis extracts, a protein signal just above the STAG3 appears, but is absent in the mutant. Anti-STAG3 antibody immunostaining of wt and *Stag3*$^{ko/ko}$ spermatocyte chromosome spreads further corroborated the absence of STAG3 in *Stag3*$^{ko/ko}$ spermatocytes (Fig 1D). In addition, cohesin immunoprecipitation (IP) affirmed the lack of STAG3 protein (see below).

Meiotic arrest in STAG3-deficient spermatocytes

To determine the stage of meiotic arrest, testis sections were prepared from STAG3-deficient and STAG3-proficient mice and stained for the AE and SC component SYCP3. The sections were also stained for γH2AX, which marks unsynapsed regions of chromosomes, and with DAPI (Fig 2A; Supplementary Fig S2 provides examples of individual *Stag3*$^{ko/ko}$ tubules and their staging). The diameter of the tubules of *Stag3*$^{ko/ko}$ mice was reduced by about half. *Stag3*$^{ko/ko}$ testis tubules in stages I and IV of the seminiferous epithelium cycle harbored cells that showed some patches of SYCP3 staining and of γH2AX. Generally, the signal intensity for γH2AX decreased with progression from stages I to IV, and thus, we consider cells with less widespread γH2AX signals more advanced. As visible in Fig 1C, no or only very short SYCP3-containing axial structures were observed in the *Stag3*$^{ko/ko}$ cells of any stage. The presence of SYCP3 indicated cells in leptonema and possibly subsequent stages. The absence of AEs, however, renders precise staging of the cells based on chromosome structure difficult. Therefore, we also analyzed the developmental stages of individual tubules based on their cell associations (Supplementary Fig S2). Progression up to tubular stage IV was observed and was not grossly perturbed. Analysis of the first wave of meiosis in young males also showed spermatocytes at days 11, 13, and 15 pp, when they would have normally reached late zygonema and are close to juvenile stage IV. *Stag3*$^{ko/ko}$ tubules beyond stage V only showed one cell layer. For example, in stage VI tubules only spermatogonia B type cells and no mid-pachytene cells were seen, which would be expected in wt

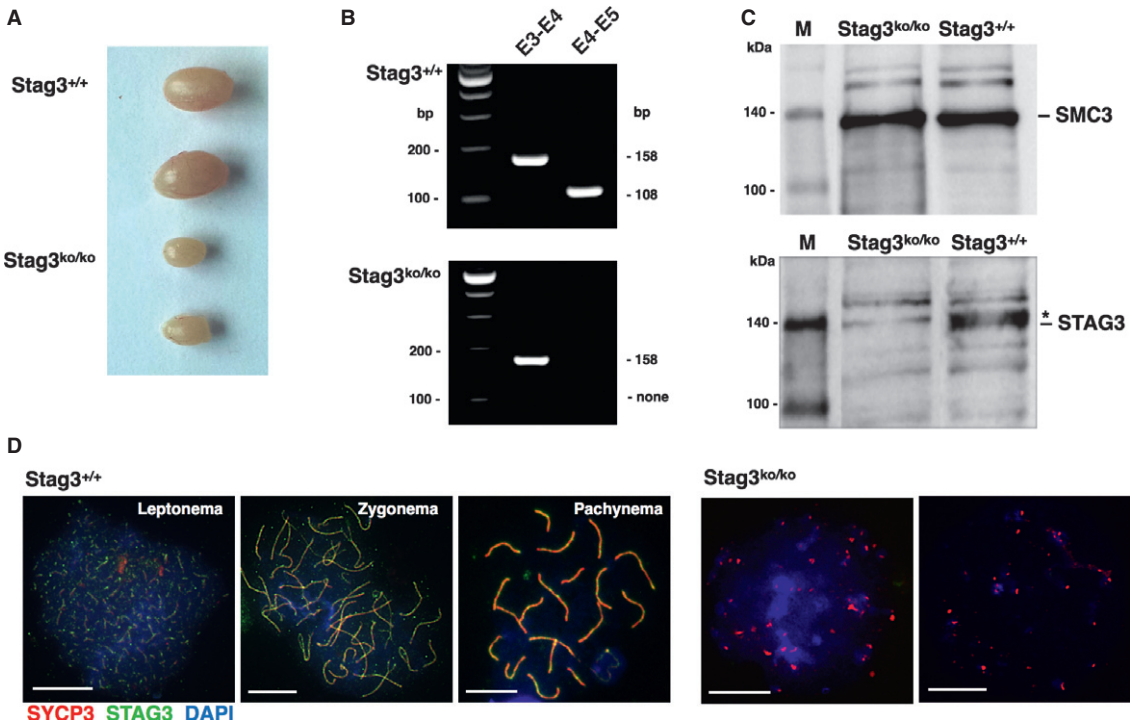

Figure 1. Characterization of spermatogenesis in *Stag3*$^{ko/ko}$ mice.

A Testis samples from wt (*Stag3*$^{+/+}$) and *Stag3*$^{ko/ko}$ mice, 40 days of age.

B RT-PCR analysis of testis mRNA from wt (*Stag3*$^{+/+}$) and *Stag3*$^{ko/ko}$ mice. The primer pairs are shown indicating the respective exons (E3, E4, E5); the expected size (bp) of the PCR products is provided.

C Immunoblot of testis nuclear extracts of the indicated mice, probed with anti-STAG3 or anti-SMC3 antibody as indicated. The anti-STAG3 antibody recognizes a specific band corresponding to the predicted molecular weight (141 kDa) of STAG3, which was present in wt but absent in *Stag3*$^{ko/ko}$ extracts. An unspecific band is marked by an asterisk. A gel was loaded in parallel using the same extracts, and the corresponding membrane was probed with an antibody directed against SMC3, which has the same predicted molecular weight (141 kDa). The pictures are representative of three independent experiments. M = biotinylated protein marker.

D Immunofluorescence staining of spermatocyte chromosome spreads of wt and *Stag3*$^{ko/ko}$ mice, probed with anti-SYCP3 antibody for AEs and SCs and anti-STAG3; nucleic acids were stained with DAPI. The stages of wt prophase I spermatocytes are indicated, and two examples of *Stag3*$^{ko/ko}$ chromosome spreads are provided. Size bars indicate 10 μm.

Source data are available online for this figure.

tubules at this stage. *Stag3*$^{ko/ko}$ tubules in stage VIII and beyond showed only mildly SYCP3-positive pre-leptotene or leptotene cells, but late pachytene or diplotene cells were absent. Stage I tubules showed early pachytene cells only (besides somatic cells present in all tubules). Stage II-III and stage IV *Stag3*$^{ko/ko}$ tubules displayed immature spermatogonia, and SYCP3-positive, γH2AX-positive cells, which correspond to early pachytene cells. Thus, spermatogenesis halts at tubular stage IV to the latest.

Together, the chromosomal stage can be described as leptotene-like, the most advanced tubular stage as stage IV, which in wt mice harbors early to mid-pachytene cells. In the following, we use the term 'leptotene-like' for the mutant spermatocytes and thus refer to the lack of AEs, although the cells and chromosomes clearly have an appearance that is very different from normal leptonema.

Deficient chromosome axis formation in *Stag3*$^{ko/ko}$ spermatocytes

Immunostaining of chromosome spreads from *Stag3*$^{ko/ko}$ spermatocytes using an anti-SYCP3 antibody confirmed a major deficiency of spermatocytes to form AEs, as only dot-like structures and sometimes short stretches were observed, which may resemble extremely short AEs, although they may be assemblies of several dots (Fig 2B). In cells that seemed less advanced, SYCP3 staining was either diffuse or appeared in aggregates of various shapes. Some cells displayed 40 SYCP3 spots of which some were slightly elongated, and other cells displayed fewer SYCP3 spots, often between 10 and 40 round spots. We considered the *Stag3*$^{ko/ko}$ cells which showed the most defined SYCP3 structures as most advanced. This also agrees with the weak SYCP3 staining in tubules at stage VIII and beyond, which would show leptotene and zygotene spermatocytes and the more intense SYCP3 in stages I to IV, which would show pachytene cells in wt. In wt spermatocytes, the staining pattern of the phosphorylated form of H2AX (γH2AX) becomes more compact as most double-strand breaks (DSBs) are repaired and homologous chromosomes start to synapse in zygonema, and in pachynema, γH2AX is confined to the sex body, the particular chromatin comprising the X and Y chromosomes, which are only paired in a very short region (Fig 2C). While there are almost no AEs in *Stag3*$^{ko/ko}$ cells and thus no synapsis and no synapsis-associated disappearance of γH2AX from the autosomes, the γH2AX

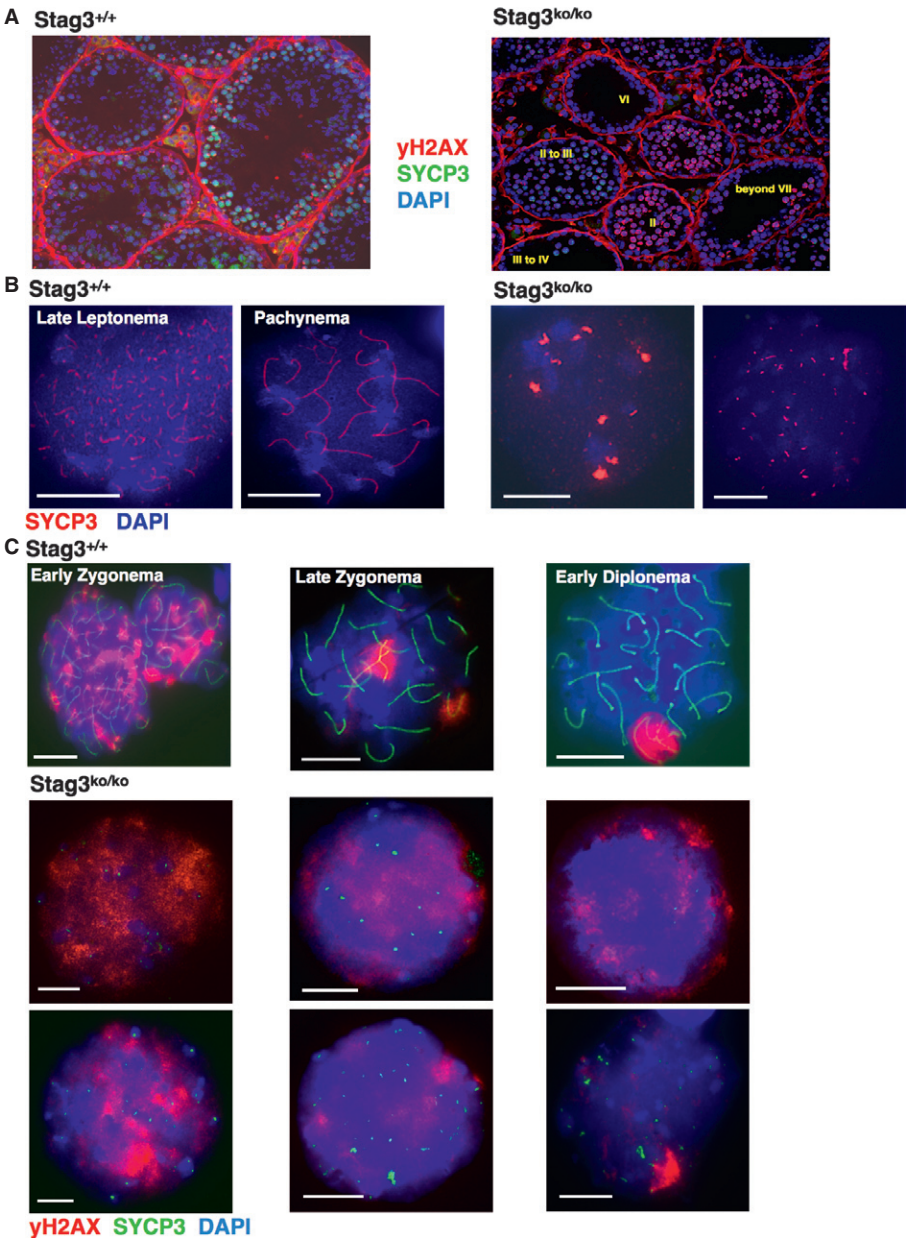

Figure 2. Axial element (AE) formation requires STAG3.

A Immunofluorescence staining of testis sections of wt and *Stag3*$^{ko/ko}$ mice, probed with anti-SYCP3 and anti-γH2AX; nucleic acids are stained with DAPI.

B Immunofluorescence staining of spermatocyte chromosome spreads of wt and *Stag3*$^{ko/ko}$ mice, probed with anti-SYCP3 antibody for AEs and synaptonemal complexes; nucleic acids were stained with DAPI. The stages of wt prophase I spermatocytes are indicated, and two examples of *Stag3*$^{ko/ko}$ chromosome spreads showing different SYCP3 staining patterns are provided. Size bars indicate 10 μm.

C Immunofluorescence staining of spermatocyte chromosome spreads of wt and *Stag3*$^{ko/ko}$ mice, probed with anti-SYCP3 and anti-γH2AX; nucleic acids were stained with DAPI. The stages of wt prophase I spermatocytes are indicated, and six examples of *Stag3*$^{ko/ko}$ chromosome spreads showing different staining patterns are provided. In agreement with the analysis of the testicular sections, we assume those cells that show the most developed albeit very small SYCP3-positive axis-like structures and the least γH2AX staining to be the most advanced. These leptotene-like cells typically show up to 40 separate SYCP3-positive dots or very short axial structures (n = 65). Size bars indicate 10 μm.

staining pattern becomes generally more compact also in *Stag3*$^{ko/ko}$ cells as these cells progress (Fig 2C, see also Fig 2A and Supplementary Fig S2), and sometimes single clouds of γH2AX are even observed. This is consistent with cell development up to stage IV.

The protein SYCP1 marks synapsed chromosomes, that is, the SC. Co-staining of wt spermatocyte chromosome spreads for SYCP1 and SYCP3 reveals axes that are unsynapsed (SYCP3-positive only) and those that are synapsed (positive for both proteins). Analysis of wt and *Stag3*$^{ko/ko}$ chromosomes showed the expected pattern in wt samples. SYCP1 signals were detected in at least half of the *Stag3*$^{ko/ko}$ cells. Figure 3A shows examples of cells without and with increasing number of SYCP1 signals, and Supplementary Fig S3 provides

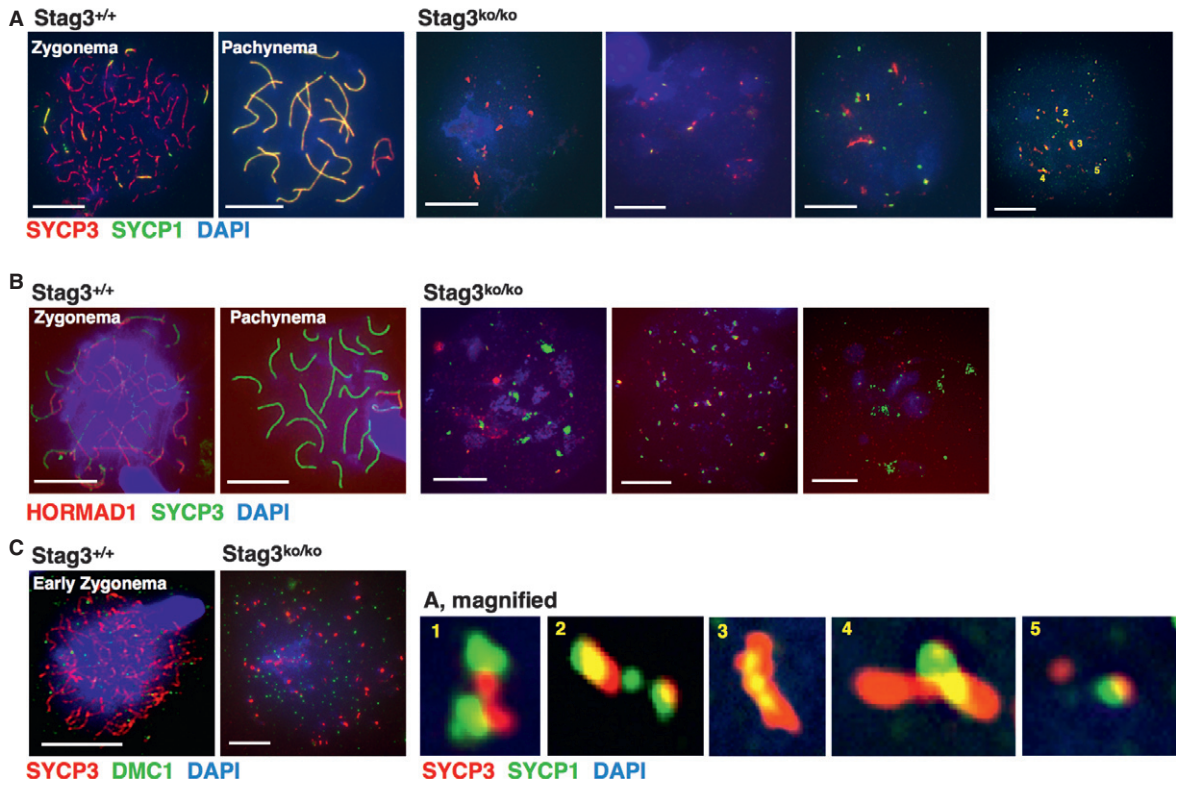

Figure 3. STAG3 and synapsis-related proteins.

A Immunofluorescence staining of spermatocyte chromosome spreads of wt and *Stag3*$^{ko/ko}$ mice, probed with anti-SYCP3 for axial elements (AEs) and anti-SYCP1 for synapsed axes; nucleic acids were stained with DAPI. Four examples of *Stag3*$^{ko/ko}$ nuclei are shown, representing different levels of SYCP1 staining. Five SYCP3/SYCP1 structures are shown magnified at the bottom of the figure and are numbered.

B Immunofluorescence staining of spermatocyte chromosome spreads of wt and *Stag3*$^{ko/ko}$ mice, probed with anti-SYCP3 for AEs and anti-HORMAD1 for unsynapsed axes; nucleic acids were stained with DAPI. Three examples of *Stag3*$^{ko/ko}$ spreads are shown, displaying different levels of HORMAD1 staining, including occasional aggregates and local accumulation.

C Immunofluorescence staining of spermatocyte chromosome spreads of wt and *Stag3*$^{ko/ko}$ mice, probed with anti-SYCP3 for AEs and anti-DMC1 for double-strand break repair foci.

Data information: nucleic acids were stained with DAPI. Size bars indicate 10 μm.

single-color images. In the cells showing the most SYCP1 signals, many but not all SYCP1 spots co-localized with SYCP3. They often located in very close proximity but did not perfectly co-localize as shown in magnified examples (Fig 3A, bottom). Many SYCP3 spots also did not co-localize with SYCP1 signals. At least the non-co-localizing spots may represent unspecific deposits of SYCP1 protein, that is, SYCP1 not associated with an axial structure. Among the SYCP1-/SYCP3-positive spots, some showed partial or full co-localization, but appeared as single dots or short rows of dots that may indicate either unspecific co-deposits or failed initiation sites where building an SC-like structure was initiated but failed. The data confirm the absence of SCs in *Stag3*$^{ko/ko}$ spermatocytes.

In wt meiocytes, HORMAD1 associates with AEs in leptonema and remains bound as long as chromosomes stay unsynapsed (Wojtasz *et al*, 2009; Fukuda *et al*, 2010). We analyzed the association of HORMAD1 with wt and *Stag3*$^{ko/ko}$ spermatocyte chromosomes to determine whether HORMAD1 binds to chromosomes in the absence of STAG3, that is, of axes and of synapsis (Fig 3B; Supplementary Fig S3). HORMAD1 associated with *Stag3*$^{ko/ko}$ chromatin in many dots, some more intense than others. The most intense HORMAD1 signals co-localized with a fraction of the SYCP3 dots or very short filaments, but did not co-localize with larger aggregates. Some of the co-localization may happen by chance considering the widespread distribution of HORMAD1. Thus, HORMAD1 preferentially localizes to SYCP3 dots and miniature axes in the absence of STAG3. This also supports the notion that the large SYCP3 signals are aggregates and not axis-containing structures.

Since very little if any AEs and no SCs are formed, we wondered whether meiotic DSBs would be generated and processed in *Stag3*$^{ko/ko}$ spermatocytes. Staining for DMC1, a meiosis-specific recombinase that contributes to repair of meiotic DSBs by homologous recombination (Habu *et al*, 1996; Pittman *et al*, 1998; Yoshida *et al*, 1998), showed numerous foci distributed throughout the chromatin in *Stag3*$^{ko/ko}$ spermatocytes (Fig 3C, Supplementary Fig S3). Thus, DNA DSB and DMC1 foci formation does not require STAG3. Without AEs, no accumulation of foci on axes can occur and the DSBs cannot be processed since the homologous partner chromosome is not available as the two homologous pairs of sister chromatids have not synapsed. Without axis co-localization, it is difficult to precisely count the number of DMC1 foci, but estimates are between 100 and 200 in *Stag3*$^{ko/ko}$ cells considered most advanced. This large number

of DMC1 signals in *Stag3*$^{ko/ko}$ cells—in early pachytene wt cells, there are <40 foci left, all localizing to the SCs—may indicate a deficiency in processing the DSBs or a failure to reach this stage. Analysis of DMC1 foci in spermatocytes derived from 11- and 13-day-old mice, when in wt the spermatocytes are in late leptonema or zygonema, respectively (Supplementary Fig S4), showed a similar presence of DMC1 foci in *Stag3*$^{ko/ko}$ cells at both time points. In the very rare cells which show some axis-like structures (one example is shown in Supplementary Fig S4), some DMC1 foci are associated with these axes, suggesting that STAG3 is not required for axis association of DMC1.

Centromere and telomere cohesion is impaired in *Stag3*$^{ko/ko}$ spermatocytes

Since SYCP3 in wt cells localizes all along the axes including close to the centromeres, we analyzed whether many of the approximately 40 SYCP3 signals observed in stag3$^{ko/ko}$ cells, which often appear in DAPI-intense heterochromatic regions, represent centromeres reflecting 40 unsynapsed pairs of sister chromatids. Immunostaining using anti-centromere antibodies (ACA) revealed that on average 71% (n = 18) of the SYCP3 signals in stag3$^{ko/ko}$ cells are very close to or partially overlap with a centromere signal (Fig 4A). This ratio varies considerably between individual cells, possibly reflecting different stages of development. In almost all of these cases, the SYCP3 signal does not completely overlap with the centromere signal but localizes to the pericentric heterochromatin with partial overlap to the inner centromere signal. When two centromere signals are observed next to each other, the SYCP3 often appears as very small extended structures between the signals or on their edges. Examples are shown in Fig 4A. In some cells, the centromeres cluster in groups of up to ten, and many but not all of these clusters contain some SYCP3. Larger, irregularly formed SYCP3 aggregates are typically not associated with centromeres, but small SYCP3 dots and miniature axes are. These data suggest that remnants of specific SYCP3 structures deposit preferentially at centromeres, possibly indicating vain attempts to initiate AE formation.

To assess whether depletion of STAG3 affects centromeric sister chromatid cohesion, we counted the number of signals obtained by ACA staining. In wt cells, 20 centromere signals are observed in pachynema. Given the absence of synapsis in *Stag3*$^{ko/ko}$ cells, intact centromeric cohesion would show 40 centromere signals, whereas a complete loss of centromeric cohesion would yield 80 distinct signals. The average number of clearly separated centromere signals in *Stag3*$^{ko/ko}$ spermatocytes was 55 ± 8 (n = 36). This shows loss of centromere cohesion for some but not all chromosomes (Fig 4A and Supplementary Fig S5A).

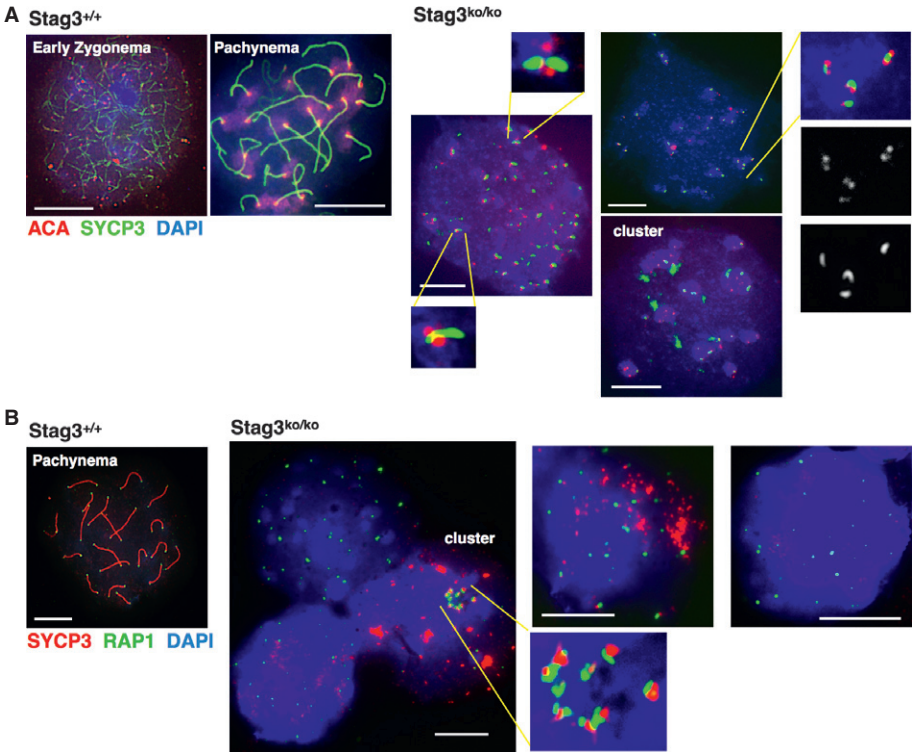

Figure 4. Centromeres and telomeres in *Stag3*$^{ko/ko}$ spermatocytes.

A Immunofluorescence staining of spermatocyte chromosome spreads of wt and *Stag3*$^{ko/ko}$ mice, probed with anti-SYCP3 and anti-centromere antibody (ACA); nucleic acids were stained with DAPI. Three examples of *Stag3*$^{ko/ko}$ spreads are shown to indicate centromere cluster formation and to highlight partial co-localization of SYCP3 with centromeres and the structures of these regions. Three areas are provided as magnified excerpts. Size bars indicate 10 μm.

B Immunofluorescence staining of spermatocyte chromosome spreads of wt and *Stag3*$^{ko/ko}$ mice, probed with anti-SYCP3 and anti-RAP1 to stain telomeres; nucleic acids were stained with DAPI. Three examples of *Stag3*$^{ko/ko}$ spreads are shown to represent different stages and to show an example of telomere cluster formation, which is shown in a magnified excerpt as well. Size bars indicate 10 μm.

Cohesin SMC1β protects telomeres, which suffer several kinds of large defects in the absence of SMC1β (Adelfalk *et al*, 2009). Since STAG3 associates with SMC1β (Prieto *et al*, 2001), we asked whether telomeres are affected by the absence of STAG3. To evaluate telomeric structure and sister chromatid cohesion, we stained telomeres by using anti-RAP1 antibody (Fig 4B). In prophase I, meiocytes contain 80 chromatids and thus 160 telomeres. If all sister chromatids are in cohesion, 80 telomere signals would be expected. If all pairs of sister chromatids were completely synapsed, 40 telomere signals are to be seen. In *Stag3*$^{ko/ko}$ chromosome spreads, more than 40 signals are observed, indicative of synapsis failures. It is not possible, however, to very precisely count the numbers of RAP1 foci since in some cells they assemble into clusters of often more than 10 foci, on some SYCP3-positive miniature axes or dots the telomere signals may be on top of each other, and in some spreads, several signals of different intensities lie next to each other. These could be telomeres of separate chromosomes that associate or could indicate a loss of telomeric cohesion. Nevertheless, counting RAP1 signals in those cells that do not show large clusters revealed up to 114 signals per cell (Supplementary Fig S5B; $n = 14$), but this is likely a significant underestimation. This suggests that telomeric sister chromatid cohesion is impaired in the absence of STAG3. Individual RAP1 foci or clusters did not always overlap with SYCP3 signals, suggesting that some telomeres may associate with each other without the formation of SYCP3-containing structures. SYCP3 signals were often detected in clusters of RAP1 foci reminiscent of telomere bouquets, where the chromosome ends are closely next to each other. This suggests that telomeres can still cluster as they do in wt in late leptonema/early zygonema (Scherthan, 2001; Siderakis & Tarsounas, 2007). Clustering of *Stag3*$^{ko/ko}$ telomeres indicates that the cells reach at least late leptonema. These results were confirmed by telomere-FISH (Supplementary Fig S6), which also showed numbers of telomere signals up to 117 and clustered telomeres. The average number of FISH telomere signals in cells which did not show clusters was 74 ($n = 23$). No extended stretches of telomere signals or telomere bridges were seen even in the most advanced cells. This contrasts SMC1β-deficient meiocytes (Adelfalk *et al*, 2009), although these cells advance further than *Stag3*$^{ko/ko}$ cells to a late zygotene/early pachytene-like chromosome structure with almost complete synapsis in some cases.

Cohesin proteins in *Stag3*$^{ko/ko}$ spermatocytes

Since sister chromatid cohesion is not entirely lost, some cohesin complexes ought to be present in *Stag3*$^{ko/ko}$ spermatocytes. To test this, we stained *Stag3*$^{ko/ko}$ spermatocyte chromosome spreads with an anti-SMC3 antibody, since SMC3 represents the only cohesin subunit present in all cohesin complexes (Fig 5A). In wt cells, SMC3 localizes along the entire AEs and SCs. In *Stag3*$^{ko/ko}$ spermatocytes with no AEs present, SMC3 localized in a dotty pattern diffusely

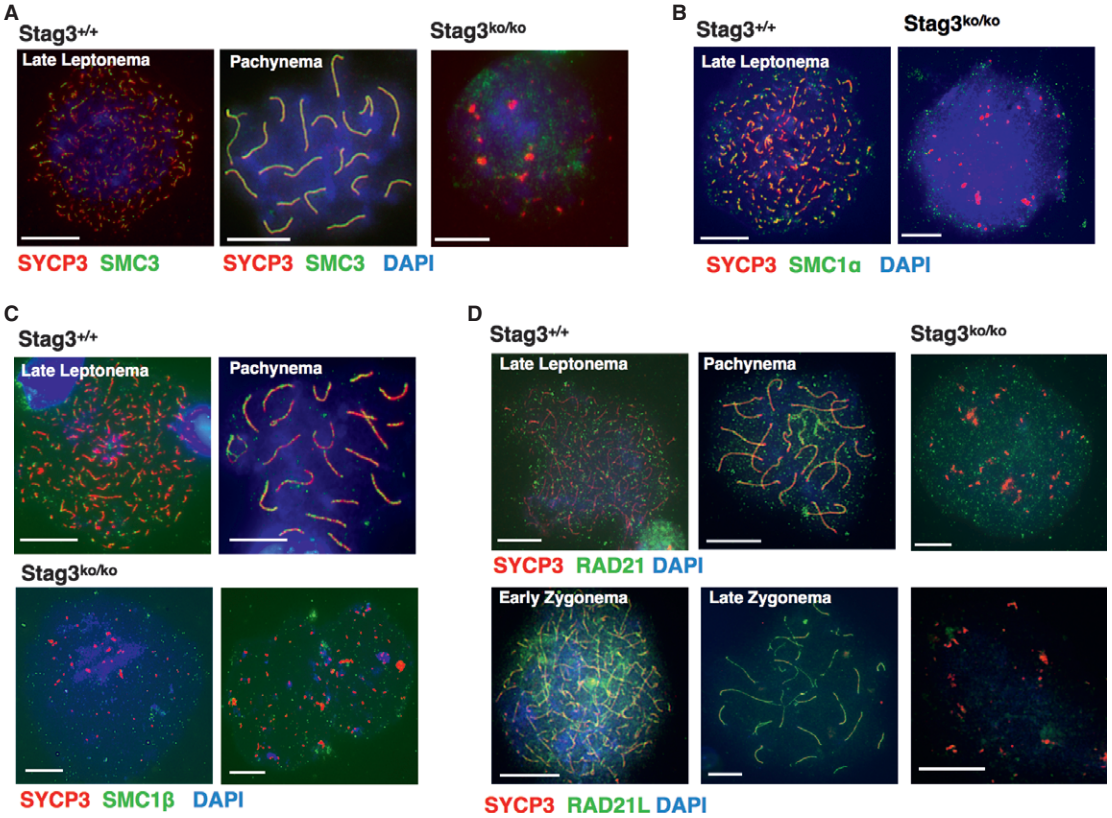

Figure 5. Cohesin proteins in *Stag3*$^{ko/ko}$ spermatocytes.

A–D Immunofluorescence staining of spermatocyte chromosome spreads of wt and *Stag3*$^{ko/ko}$ mice, probed with (A) anti-SYCP3 and anti-SMC3; (B) anti-SYCP3 and anti-SMC1α; (C) anti-SYCP3 and anti-SMC1β; (D) anti-SYCP3 and anti-RAD21 or anti-RAD21L. Nucleic acids were stained with DAPI. Size bars indicate 10 μm.

throughout the DAPI-stained chromatin. No particular accumulation in certain nuclear regions was visible, suggesting that cohesin complexes are evenly distributed and may to some extent still support sister chromatid cohesion. Accordingly, the partner SMC proteins, either SMC1α or SMC1β, were also present in *Stag3*$^{ko/ko}$ spermatocytes in a diffuse, dotty pattern (Fig 5B,C). Staining for two kleisins, RAD21 and the meiosis-specific RAD21L, showed that both proteins are present in *Stag3*$^{ko/ko}$ spermatocytes (Fig 5D), although the signals for RAD21L were weak.

To further analyze cohesin complexes in wt and mutant spermatocytes and to confirm the above findings, we performed immunoprecipitation experiments. We used anti-SMC1β antibody to ensure precipitation only from spermatocytes, for SMC1β is meiosis-specific, and to capture the majority of meiotic complexes. Figure 6A shows that SMC1β is present in wt and *Stag3*$^{ko/ko}$ spermatocytes and can readily be precipitated. Both SMC3 and REC8 co-precipitate, but there is much less REC8 in extracts and precipitates from the mutant cells, perhaps indicating decreased stability. There is no RAD21 co-precipitating. A wt-like co-precipitation signal appeared in *Stag3*$^{ko/ko}$ spermatocytes samples for RAD21L. STAG3 is absent in the anti-SMC1β IP from *Stag3*$^{ko/ko}$ spermatocytes, but is clearly present in the IP from wt cells. SA1 and SA2 are also co-precipitated by anti-SMC1β from wt cells, although rather weakly. Interestingly, this signal is much stronger in the anti-SMC1β IP from *Stag3*$^{ko/ko}$ spermatocytes.

In addition, we analyzed whether cohesins are chromatin-associated in testes from wt and *Stag3*$^{ko/ko}$ mice and performed differential salt extraction with increasing salt concentrations of 0, 25, and 250 mM ammonium sulfate (Fig 6B). SMC3 and SMC1α are present in somatic and meiotic cells of the testis, and SMC1β and REC8 only in spermatocytes. In wt and *Stag3*$^{ko/ko}$ samples, at least a substantial fraction if not nearly all of each of these cohesins dissociated from chromatin at high salt, indicative of rather tight chromatin association. A fraction of REC8 was extracted with 25 mM salt or even leaked out of nuclei without any extra salt added. Together, these results show that cohesin complexes still exist on spermatocyte chromosomes in the absence of STAG3.

Deficiencies in *Stag3*$^{ko/ko}$ oocytes largely parallel those in spermatocytes

No oocytes were found in adult *Stag3*$^{ko/ko}$ mice of ages 6 weeks and higher. As we observed major defects in early male prophase I, we analyzed embryonic oocytes at embryonic day 15 when cells of leptonema to the very late stage of zygonema can be found in wt mice (Fig 7). Similar to spermatocytes, staining for SYCP3 in

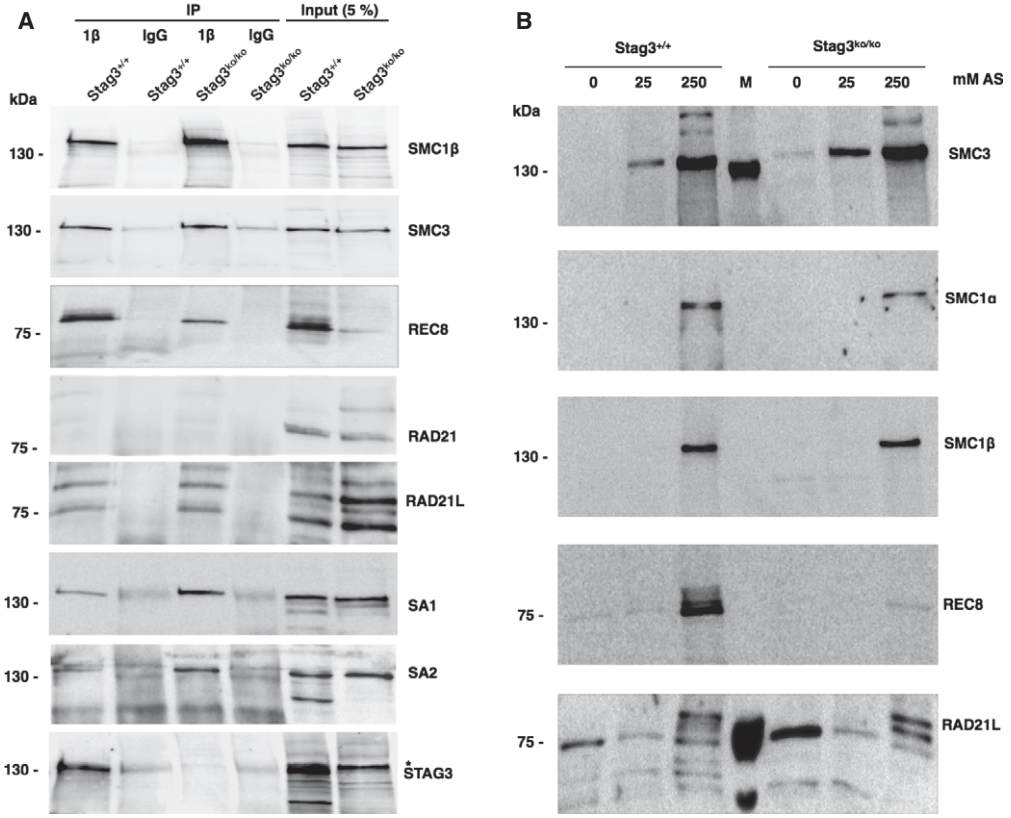

Figure 6. Cohesin proteins in wt and in *Stag3*$^{ko/ko}$ testis.

A Immunoprecipitation of cohesin complexes from wt and *Stag3*$^{ko/ko}$ testis nuclear extract using anti-SMC1β antibody (1β) or control IgG as indicated. Precipitates and 5% of input extracts are probed with the indicated antibodies for specific cohesin proteins.

B Stepwise extraction of proteins from wt and in *Stag3*$^{ko/ko}$ testes nuclei using 0, 25, and 250 mM ammonium sulfate (AS) as indicated. Extracts were immunoprobed using the antibodies indicated on the right. *Unspecific band; M = marker; kDa numbers refer to marker signals.

Source data are available online for this figure.

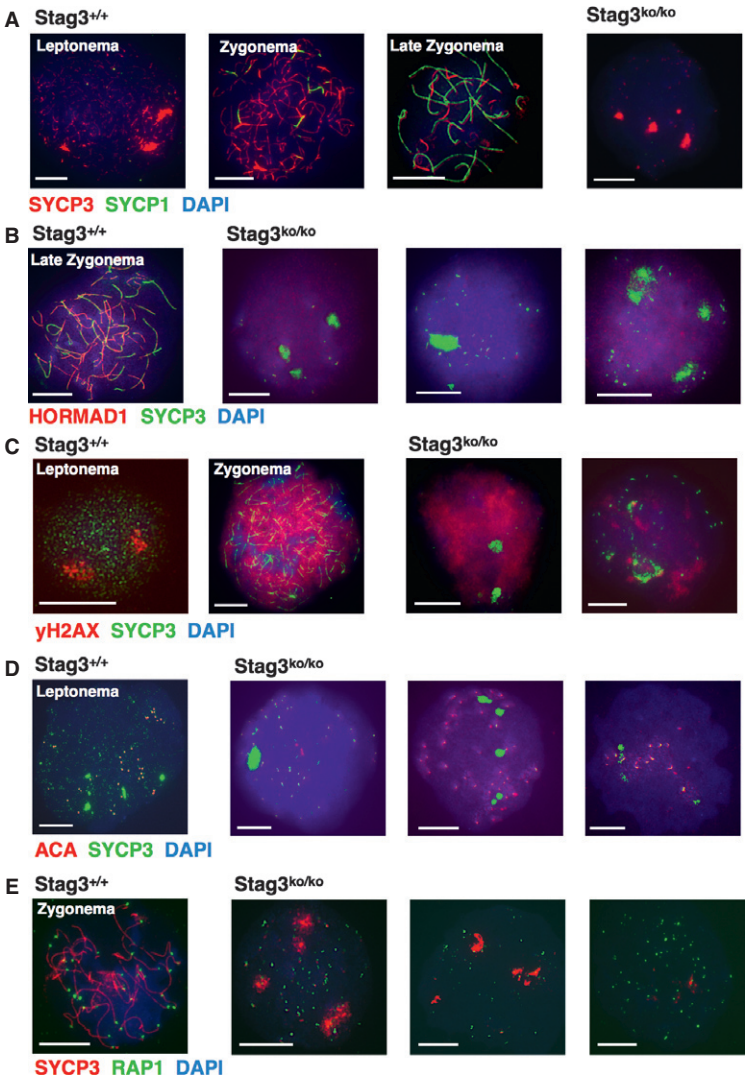

Figure 7. Analysis of embryonic day 15 oocyte chromosomes of wt and *Stag3*$^{ko/ko}$ mice.

A–E Immunofluorescence staining of chromosome spreads with anti-SYCP3 and (A) SYCP1 as a synapsis marker; (B) HORMAD1 as a marker for unsynapsed regions; (C) γH2AX to show progression through the initial stages of prophase I; (D) anti-centromere antibody ACA; (E) anti-RAP1 to visualize telomeres. Size bars indicate 10 μm.

embryonic oocytes showed the absence of chromosome axes or extremely short axis-like structures and occasionally SYCP3 aggregates. SYCP1 signals were very weak or absent in about 20% of the cells, and in most of the other cells, small dots of SYCP1 appeared, which overlapped with SYCP3 in about 40% of the cases (Fig 7A).

HORMAD1 localizes diffusely to the entire chromatin and also overlaps with SYCP3, which can hardly be avoided as HORMAD1 is widespread and thus there is no indication for a specific structure (Fig 7B). The γH2AX was either present in large quantities covering almost the entire chromatin, or in smaller clouds, particularly in those cells, which had formed many SYCP3 spots and a few very short SYCP3 filaments (Fig 7C). We consider cells that have many defined SYCP3 spots and little γH2AX as most advanced.

Similar to spermatocytes, many centromere signals overlapped with SYCP3 signals, and in some *Stag3*$^{ko/ko}$ oocytes, likely of the more advanced early zygotene stage, centromere clusters were observed (Fig 7D). The number of centromere signals varied between at least 41 and 68 and was never 40 or less (n = 12). Like for the spermatocytes, these numbers are likely underestimates since only clearly identifiable spots were counted and some of the spots presented in clusters. Examples of images used for counting are provided in Supplementary Fig S7A. Wt oocytes showed 38–40 centromere signals, illustrating the difficulty to identify all centromeres.

Telomere signals obtained by anti-RAP1 staining varied greatly in numbers, similar to observations made for spermatocytes. Figure 7E shows three examples of *Stag3*$^{ko/ko}$ oocytes of different stages (see Supplementary Fig S7B for RAP1 inverted color spots used for counting). The numbers of clearly distinct RAP1 spots were above 80, between 83 and 122, but again are likely underestimates since telomeres cluster and signal intensities vary between spots. Telomere signals often came in pairs, which suggests a loss of

cohesion at least in the case of non-clustered telomeres. If synapsis completely fails, which is highly likely given the absence of axes, 80 telomere spots are expected; if in addition telomere sister chromatid cohesion completely fails, 160 spots are expected. Any number above 80 indicates at least partial loss of telomere cohesion. Like in spermatocytes, no telomere extensions or bridges or other telomere defects were seen. Thus, *Stag3*$^{ko/ko}$ oocytes suffer from at least a partial loss of centromeric and telomeric sister chromatid cohesion.

Cohesin proteins such as SMC3, SMC1α, SMC1β, RAD21, and low levels of RAD21L were detected in *Stag3*$^{ko/ko}$ oocytes spreads and localized diffusely in dotty patterns throughout the chromatin (Supplementary Fig S8).

Discussion

Similar to other cohesin mouse mutants, spermatogenesis in *Stag3*$^{ko/ko}$ mice is aborted at a leptotene-like stage based on the absence of AEs. According to the tubular stage, the increased formation of SYCP3 dot-like structures and miniature filaments as well as of increasing spotty SYCP1 deposits, the reduction in γH2AX staining, and the presence of telomere clusters, we suggest that the most advanced cells reach late zygonema defined as a tubular developmental stage. If, however, staging relies exclusively on chromosome features, and thus clearly visible extended AEs that are undergoing synapsis are to be considered the major or even sole defining parameter for 'zygonema', then the *Stag3*$^{ko/ko}$ spermatocytes shall be called leptotene-like cells. The terminology is not clearly defined in such cases.

The analysis of male and female meiocytes deficient in the only meiosis-specific STAG cohesin protein, STAG3, revealed a drastic phenotype in both sexes: the virtual absence of AEs and thus of SCs. While dots or aggregates of SYCP3 are seen in many cells, only few *Stag3*$^{ko/ko}$ meiocytes show one or a small number of miniature axis-like structures, which may constitute AE initiator units or unspecific aggregates of SYCP3, which tends to form filamentous structures by itself (Yuan *et al*, 1996). SYCP3 is particularly visible on clustered centromeres or telomeres. The centromere-associated SYCP3 signals do not cover the entire centromere but rather extend from the pericentromeric region, reaching partially into the inner centromeric region stained by ACA. Very little of the SC-specific protein SYCP1 is present in *Stag3*$^{ko/ko}$ meiocytes, and if present, SYCP1 often but not always overlaps with SYCP3 in small dot-like structures. We do not consider this an indication for synapsis but rather as unspecific deposits. DSBs are still formed in the *Stag3*$^{ko/ko}$ chromatin as the staining for DMC1 foci showed. This is consistent with other cohesin deficiencies such as in the *Smc1*β$^{-/-}$ mouse (Revenkova *et al*, 2004; Biswas *et al*, 2013), where DMC1 and RAD51 foci are present, and suggests that the introduction of these breaks by SPO11 and the formation of repair foci do not depend on STAG3. The presence of high numbers of DMC1 foci may suggest that these foci are not processed, that is, the DSBs are not repaired. In wt cells at the end of zygonema, there are typically <50 DMC1 foci left, down from 120 to 200 foci present in early zygonema. Most *Stag3*$^{ko/ko}$ cells display more than 100 foci, but it is not possible to derive precise numbers for specific stages, since precise staging of individual cells is not possible. This suggests that DSBs may not be repaired efficiently, similar to delayed repair seen in *Smc1*β$^{-/-}$ spermatocytes (Biswas *et al*, 2013) or in *Rec8*$^{-/-}$ *Rad21L*$^{-/-}$ spermatocytes, which show a similar phenotype with the absence of AEs and SCs (Llano *et al*, 2012), or that it is a consequence of the cells not developing sufficiently to repair the DSBs.

The presence of γH2AX indicates unsynapsed AEs and unrepaired DSBs. With progression of synapsis in wt meiocytes, γH2AX disappears from unsynapsed chromosomes except the X and Y chromosomes, which remain largely unsynapsed. In the *Stag3*$^{ko/ko}$ meiocytes, essentially no AEs and no SCs are formed, yet γH2AX signals appear weaker and more concentrated in a few cloud-like structures when cells appear to progress as indicated by tubular stage and by increased formation of SYCP3 foci or miniature axes. This suggests that in the absence of STAG3, the ATM-mediated phosphorylation of H2AX cannot be maintained despite the failure to synapse. One may speculate that activation of ATM initially requires AEs to be formed, or the maintenance of ATM activity requires AEs and thus AE-associated proteins such as HORMAD1 (Fukuda *et al*, 2010; Daniel *et al*, 2011). HORMAD1, which normally associates with unsynapsed axes, has no axes to bind to but is still present diffusely throughout the nuclei. HORMAD1 was not reported to be analyzed in the *Rec8*$^{-/-}$ *Rad21L*$^{-/-}$ spermatocytes, which also mostly lack AEs and SCs (Llano *et al*, 2012).

While axis formation entirely depends on STAG3, sister chromatid cohesion is only partially impaired in STAG3-deficient meiocytes. The presence of an average of at least 55 separate centromeres in *Stag3*$^{ko/ko}$ meiocytes indicates that there is no synapsis between homologous chromosomes and that centromeric sister chromatid cohesion is impaired but not eradicated. Otherwise, 80 separate spots would have been observed. This observation is in agreement with the presence of sister chromatid cohesion in REC8-, RAD21L-, or SMC1β-deficient mutants, although at reduced levels (Bannister *et al*, 2004; Revenkova *et al*, 2004; Xu *et al*, 2005; Herran *et al*, 2011; Biswas *et al*, 2013), and with impaired centromeric cohesion found in oocytes of a very recently generated *Stag3* insertional mutagenesis mouse strain (Caburet *et al*, 2014). Another recent study showed that the SMC1α-based complexes present in prophase I provide a substantial fraction of centromeric sister chromatid cohesion (Biswas *et al*, 2013). Thus, SMC1α and/or SMC1β complexes containing SA1 or SA2 should provide sister chromatid cohesion in the absence of STAG3. Only a minor fraction of SMC1β is likely to associate with SA1 or SA2 in wt cells (Lee & Hirano, 2011), but this fraction appears to increase in the absence of STAG3 (Fig 6A). Thus, SA1 or SA2 complexes, either associated with SMC1α or SMC1β, support much of sister chromatid cohesion in *Stag3*$^{ko/ko}$ meiocytes, but also provide some cohesion in wt cells. In SMC1β-deficient spermatocytes, SMC1α/SA1 or SA2 complexes likely support the remaining cohesion (Biswas *et al*, 2013).

The above concerns centromeric cohesion. Telomere staining suggests that telomeric sister chromatid cohesion is not entirely abolished in *Stag3*$^{ko/ko}$ either. In *Stag3*$^{ko/ko}$ meiocytes, we observed more than 80 but never 160 telomeres identified by RAP1 staining or by telo-FISH. While we cannot exclude that some telomere signals were missed as they may have been very weak, this suggests that a substantial fraction of telomeric cohesion depends on STAG3. Together, we conclude that STAG3-type cohesin complexes play a significant role in meiotic sister chromatid cohesion.

SMC1β was found to protect telomeres from damage such as breaks, large extensions, and easily identifiable interchromosomal telomere bridges (Adelfalk *et al*, 2009). No such damage was seen

upon RAP1 or FISH staining of *Stag3*$^{ko/ko}$ chromosomes. This may suggest that STAG3 is at least not prominently involved in telomere protection and that a different SMC1β-type complex fulfills this role, perhaps a complex with SA1 or SA2. However, the mutant cells remained in a leptotene-like chromosomal stage. Telomere damage such as seen in SMC1β-deficient zygotene and early pachytene spermatocytes (Adelfalk *et al*, 2009) may therefore not be present or visible in *Stag3*$^{ko/ko}$ spermatocytes.

The previously described meiosis-specific cohesin mutants deficient in REC8, RAD21L, or SMC1β (Bannister *et al*, 2004; Revenkova *et al*, 2004; Xu *et al*, 2005; Herran *et al*, 2011) still form AEs and SCs although these are shorter than in wt and synapsis is incomplete. In contrast, STAG3-deficient spermatocytes and oocytes do not form AEs. This suggests that STAG3-containing cohesin complexes are most important for axis formation and that STAG3 is present in several different types of cohesin complexes in meiocytes. An almost complete absence of chromosome axes was reported in *Rec8*$^{-/-}$ *Rad21L*$^{-/-}$ spermatocytes (Llano *et al*, 2012). Together with the results reported here, this suggests that these two kleisins are part of the major forms of cohesin complexes acting in axis formation and that these are associated with STAG3. This is in agreement with the very weak signals for RAD21 observed before pachynema in wt meiocytes and its absence in anti-SMC1β immunoprecipitates (Fig 6). Deficiency in STAG3 would affect RAD21L- and REC8-based complexes and thus elicit a similar phenotype as the 'double-knockout'. However, the continued presence of cohesin on *Stag3*$^{ko/ko}$ but not on *Rec8*$^{-/-}$ *Rad21L*$^{-/-}$ chromosomes (Llano *et al*, 2012), and the impairment of sister chromatid cohesion only in the former but not in the latter mutant, illustrates that other cohesin protein combinations exist.

The cohesin proteins present in *Stag3*$^{ko/ko}$ meiocytes localize diffusely throughout the chromatin. There is no axis to associate with, but the presence of all three SMC proteins, SMC1α, SMC1β and SMC3, suggests that a population of cohesin complexes exist in the absence of STAG3. These include REC8 and RAD21L kleisins, although the stability of REC8 may be reduced in the absence of STAG3. Looser association of REC8 with testis chromatin is also indicated by the differential salt extraction experiment, where more REC8 appeared in the *Stag3*$^{ko/ko}$ low-salt fractions. To form a four-subunit cohesin complex, these complexes would have to associate with SA1 or SA2. However, no interaction of SMC1β or REC8 or RAD21L with SA1 or SA2 was observed (Ishiguro *et al*, 2011; Lee & Hirano, 2011). We observed a rather weak but clear signal for SA1 and SA2 co-precipitating with SMC1β in wt, and these signals were enhanced in the absence of STAG3. One may speculate that in the absence of STAG3, expression of SA1 and SA2 is upregulated in spermatocytes (not visible in total testis extract), or its stability is enhanced through association with cohesin complexes typically associated with STAG3, or that SA1 and SA2 can more efficiently associate with SMC1β complexes in the absence of STAG3, which may bind with the highest affinity.

SMC1α-based complexes are most clearly observed in early prophase I and fade away when cells progress toward metaphase I (Eijpe *et al*, 2000). The presence of SMC1α-based complexes is consistent with the existence of considerable sister chromatid cohesion at centromeres and along chromosome arms in early prophase I of *Smc1β*$^{-/-}$ meiocytes (Revenkova *et al*, 2004; Biswas *et al*, 2013). IP data from several laboratories suggest that SMC1α can associate with either RAD21 or RAD21L, at least in testis nuclear extracts or somatic cell overexpression systems (Gutierrez-Caballero *et al*, 2011; Ishiguro *et al*, 2011; Lee & Hirano, 2011), although one study suggested that SMC1α does not associate with RAD21L (Ishiguro *et al*, 2011). The presence of AEs and SCs in *Smc1β*$^{-/-}$ meiocytes suggests that SMC1α-based complexes significantly contribute to AE/SC formation, since cohesin is required for AE/SC formation as this study and the analysis of *Rec8*$^{-/-}$ *Rad21L*$^{-/-}$ spermatocytes (Llano *et al*, 2012) show. An association of the SMC1α/RAD21 complex is consistent with anti-RAD21 IPs or pull-downs of tagged proteins, both of which precipitated STAG3 (Gutierrez-Caballero *et al*, 2011; Ishiguro *et al*, 2011). This is also consistent with co-IP experiments showing that RAD21 co-precipitates with STAG3, although very little if any SMC1α was precipitated with anti-STAG3 antibodies (Lee & Hirano, 2011). Co-precipitates from testis extracts may reflect the interaction between RAD21 and STAG3 within an SMC1β-type complex, and the interactions seen upon overexpressing tagged proteins in somatic cell lines may not necessarily occur in primary meiocytes. Whether SMC1α associates with REC8 and RAD21L is uncertain, since these associations were seen in some but not all studies (Revenkova *et al*, 2004; Ishiguro *et al*, 2011; Lee & Hirano, 2011). There is evidence though from several laboratories that SMC1β forms distinct complexes with each of the three kleisins (Revenkova *et al*, 2004; Gutierrez-Caballero *et al*, 2011; Ishiguro *et al*, 2011; Lee & Hirano, 2011). Each of these complexes is associated with STAG3, consistent with the drastic phenotypes reported here.

Notably, in an accompanying paper by Fukuda *et al*, a distinct *Stag3* mouse mutant is presented, which expresses low levels of STAG3 and shows a characteristic dosage phenotype (Fukuda *et al*, 2014). There are still AEs, but they are short; there is still a low level of synapsis, but it is aberrant, and only two of the three kleisins still localize to the chromosome axes. REC8 does not, indicating a particular requirement of STAG3 for REC8-based complexes. A few days before resubmission of this report, a publication appeared that also describes phenotypes of a mouse strain carrying a lentiviral insertion in exon 8 of the *Stag3* gene (Llano *et al*, 2014). Whether a small amount of residual STAG3 protein is present in this strain is uncertain as no immunoblotting or highly sensitive mRNA RT-PCR data were presented. The phenotype described in Llano *et al*, 2014 is more consistent with that of the report by Fukuda *et al*, since there are still small axes formed, some of which are synapsed and stained continuously for SYCP1. A partial or even complete SC was observed, unlike in the STAG3-deficient mouse strain described here. Thus, the STAG3 deficiency reported here appears to be the most severe. Other phenotypes such as partial loss of centromeric cohesion and the presence of some cohesin on spermatocytes spreads of the *Stag3* insertion mutant are consistent with those reported here.

In summary, we propose that SMC1α- and SMC1β-based cohesin complexes together determine meiotic chromosome AE formation and synapsis, and they do so mainly in association with STAG3. Meiotic sister chromatid cohesion, which as described above depends to a significant part on STAG3, is mainly supported by SMC1β-type complexes, but SMC1α complexes contribute in the initial phase of meiosis I as well. Thus, STAG3 appears to be the most important single meiotic cohesin protein. No other deficiency in a single meiosis-specific cohesin causes a phenotype as drastic as that of STAG3 deficiency.

Materials and Methods

Animals

Stag3$^{ko/ko}$ ES cells were obtained from KOMP, San Diego, USA (clone name EPD050_4_G09), and are derived from the parental ES line JM8A3.N1. The allele name is Stag3$^{tm1a(KOMP)Wtsi}$ and is named 'ko' in this communication to indicate that this is a knockout-first construct (see Supplementary Fig S1) and not a deletion allele. ES cells were injected into C57BL/6 blastocysts and the resulting mice bred to homozygosity for this locus. Genotyping was performed using the following PCR primers: primer 1: 5′-GTT ATC TAG CCA CTC ATC CAC C-3′; primer 2: 5′-CGC CTT CTT GAC GAG TTC TTC-3′; primer 3: 5′-GCA AGT GTT CTC CAC TGC TAA G-3′, and yielded the following products: Stag3 ko: primers 1 and 2 (product: 1412 bp); Stag3 wt: primers 1 and 3 (product: 1077 bp). Animals were bred and maintained under pathogen-free conditions at the Experimental Center of the Medizinisch-Theoretisches Zentrum of the Medical Faculty at the Dresden University of Technology according to approved animal welfare guidelines, permission number 24-9168.24-1/2010-25 granted by the State of Saxony.

RNA extraction and RT-PCR

A single cell suspension was obtained from whole testes using Dounce homogenization, followed by centrifugation at 600 rpm for 10 min at 4°C. One ml of TRIzol was added to the cell pellet and incubated at room temperature (RT) for 5 min, followed by 200 μl of chloroform and incubated at RT for 3 min. The mixture was centrifuged at 1,770 *g* for 15 min and the aqueous phase used for RNA precipitation with 500 μl of isopropanol followed by centrifugation at 1,770 *g* for 10 min at 4°C. The pellet was washed with 70% ethanol, dried, and resuspended in 50 μl of RNAase-free water. One μg of total RNA was used per 20 μl of reverse transcription reaction (SuperScript II, Invitrogen). The mixture was incubated for 5 min at 65°C before adding the 5× first-strand buffer and DTT (10 mM final concentration). The mixture was chilled and heated to 42°C before adding the SuperScript reverse transcription enzyme (10 u/μl final concentration). The reaction was incubated for 50 min at 42°C, followed by inactivation at 70°C for 15 min. 2 μl of the RT reaction was used as template in a standard 50 μl PCR (denaturation at 95°C for 30 s, annealing at 60.5°C for 30 s, and elongation at 72°C for 1 min).

The primers used were: E3 fwd 5′-TAGTCCCTCCACTAACTAACGAAGACAG; E4 rev 5′-CTGATTCATTCTTGCCATTCCCAC; E4 fwd 5′-GTGGGAATGGCAAGAATGAATCAG; E5 rev 5′-AGTTATCTAGCCCACTCATCCACC.

Cryosectioning of testes

Whole testes were fixed in 4% formaldehyde for 30 min, incubated in 30% sucrose for 16 h at 4°C, and immersed in O.C.T Compound (Tissue-Tek 4583) in specimen molds (Tissue-Tek 4566 Cyromold 15 × 15 × 5 mm) and frozen at −80°C. 7-μm sections were cut using a Leica CM1900 cryostat microtome and placed onto microscope slides (StarFrost K078; 76 × 26 mm). Sections were immersed in cold methanol for 10 min, then in cold acetone for 1 min, and dried for 10 min. The slides were washed in 1 × PBST (PBS plus 0.1% Tween-20), then subsequently blocked in 2% BSA in 1× PBS for 30 min, and incubated with primary antibodies at 4°C for 16 h. Primary antibodies used in this experiment were anti-SYCP3 (mouse monoclonal, hybridoma cell line supernatant) and anti-γH2AX phospho-Ser139 (1:500, mouse monoclonal IgG_1, Millipore 05-636). Slides were washed three times in 1× PBS and incubated with secondary antibodies for 1–2 h at 22°C. Slides were washed three times in 1× PBS and mounted using VectaShield mounting media (Vecta Laboratories, H-1000) containing 1 μg/ml DAPI and 24 × 50 mm coverslips (Engelbrecht, K12450, depth 0.13–0.17 mm). Testis sections were imaged using a Zeiss Axiophot microscope at 20× or 40× magnification with oil of refractive index 1.518 (Zeiss, Immersol 518 F).

Immunoblot analysis of testes extracts

For protein extraction and immunoblotting, the tunica albuginea was removed from the testes and a single cell suspension created using Dounce homogenization (loose pestle) in buffer B (5 mM KCl, 2 mM DTT, 40 mM Tris (pH 7.5), 2 mM EDTA, and protease inhibitors). Nuclear extracts were prepared essentially as described in Jessberger *et al*, 1993. In brief, nuclear membranes were broken using Dounce homogenization (tight pestle). The nuclear suspension was centrifuged at 1,180 *g* for 3 min, the nuclear pellets resuspended in buffer C (5 mM KCl, 1 mM DTT, 15 mM Tris (pH 7.5), 0.5 mM EDTA, and protease inhibitors), and nuclear proteins were extracted by adding ammonium sulfate (pH 7.4) to a concentration of 250 mM and incubating on ice for 30 min. Samples were centrifuged at 234,000 *g* for 30 min at 4°C. Supernatant was collected and protein content measured by Bradford before being stored at −20°C in Laemmli buffer for Western analysis. 5 μg of protein was run on an 8% SDS–PAGE gel, transferred to a nitrocellulose membrane, and blocked in 5% milk in PBST for 1 h at 22°C. Primary antibodies were added at 1 μg/ml in PBST for 16 h at 4°C. Primary antibodies used were as follows: rabbit anti-STAG3 (1:2000), mouse anti-SMC1β (mAb #76 or #102 at 1 μg/ml or 1:2 diluted hybridoma supernatant), and rabbit anti-SMC3 (1:1,000, Bethyl A300-060A). Membranes were washed three times in PBST and HRP-conjugated secondary antibodies were added for 1 h at 22°C in PBST. Secondary antibodies used were as follows: anti-rabbit IgG HRP (eBioscience 18-8816-31) and goat anti-mouse IgG HRP (Dianova 115-035-003). A biotinylated protein ladder (Cell Signaling Technology 7727) was loaded onto each gel and detected using an anti-biotin HRP (Cell Signaling Technology 7075). Blots were washed three times in PBST and developed using chemiluminescent HRP substrate (Millipore, WBKLS) and imaged on a Kodak ImageStation 2000MM.

Nuclear spreads and immunofluorescence

The tunica albuginea was removed from the testes, and testis tubules were incubated in 500 μl of 1 mg/ml collagenase for 10 min at 32°C. A single tubule suspension was obtained by pipetting and then centrifuged for 5 min at 380 *g* at 22°C. The pellet was resuspended in 0.05% trypsin and incubated for 5 min at 32°C with agitation of 350 rpm. Trypsin activity was neutralized by adding 200 μl of DMEM containing 10% FCS. The single cell suspension was filtrated through a 40-μm strainer by centrifugation

at 2,000 rpm for 10 s and then centrifuged at 320 *g* for 5 min at 22°C. The pellet was resuspended in 500 μl of PBS. For embryonic ovaries, a single ovary was incubated in PBS + 5 mM EDTA (pH 7.2) for 2 min at 4°C, incubated in a droplet of 1 mg/ml collagenase in 1× PBS for 2 min at 4°C, washed in 1× PBS, and macerated in 15 μl of 1× PBS. The single cell suspension was obtained by diluting the macerate 10× in PBS. 1-2 μl of single cell suspension was added to each well of a 10-well slide (Thermo Scientific, ER-308B-CE24, 10 well, 6.7 mm) containing 0.25% NP-40; cells were lysed for 2 min and fixed with 1% PFA, 5 mM sodium borate pH 8.5, 0.15% Triton-X 100. The slides were incubated in a wet chamber for 1 h, dried for 30 min to 1 h, washed two times with 0.5% Photo-Flo (KODAK, 146 4510), washed two times with PBS, dried, and stored at −20°C.

For immunofluorescence, primary antibodies used were as follows: mouse anti-SYCP3 (hybridoma supernatant), rabbit anti-SYCP3 (1:100, Novus Biologicals NB300-230), rabbit anti-STAG3 (0.2 μg/ml, Protein A-purified Ab), mouse anti-γH2AX (1:500, Millipore 05-636), mouse anti-γH2AX biotin conjugate (1:500, Millipore 16-193), rabbit anti-SYCP1 (1:100, abcam ab15090), rabbit anti-DMC1 (1:50, Santa Cruz Biotechnology sc-22768), human anti-centromere (1:200, Antibodies Incorporated 15-235-0001), rabbit anti-RAP1 (1:50, Imgenex IMG-289), rabbit anti-SMC3 (1:100, abcam ab9263), rabbit anti-SMC1α (1:100), mouse anti-SMC1β (mAb #76 or #102 at 0.5 μg/ml or 1:2 diluted hybridoma supernatant), rabbit anti-RAD21 (1:100, abcam ab992), rabbit anti-RAD21L (1:100, kindly provided by Dr A. Pendas), and guinea pig anti-HORMAD1 (1:700, gift from Dr A. Toth). Secondary antibodies were all used in 1:500 dilution as follows: Cy3 goat anti-mouse IgG (Biolegend 405309), Alexa Fluor 488 goat anti-rabbit IgG (Invitrogen A11034), Alexa Fluor 568 goat anti-guinea pig IgG (Invitrogen A11075), and Alexa Fluor 568 goat anti-human IgG (Invitrogen A21090).

Differential salt extraction and immunoprecipitation

For stepwise salt extraction of nuclei, the nuclei were first incubated for 30 min, on ice in a hypotonic buffer to allow nucleoplasmic proteins to diffuse out of the nuclei. The nuclei were then centrifuged (800 rpm, 5 min, 4°C) and the supernatant taken. The nuclei were washed once with the same buffer and same low-speed centrifugation. The nuclei were then resuspended in the same buffer with 25 mM ammonium sulfate added to extract proteins loosely bound to chromatin, and incubated for 30 min on ice. Again, the nuclei were centrifuged, the supernatant taken (25 mM fraction), washed once, and resuspended and incubated for 30 min on ice in the same buffer containing 250 mM ammonium sulfate to extract proteins tightly chromatin-associated. After centrifugation at 1,770 *g* for 10 min at 4°C to pellet the remnant nuclei, the supernatant was taken (250 mM fraction). The immunoprecipitations were performed as described in Revenkova *et al*, 2004. The primary antibodies used were the same as described above for immunofluorescence staining. Protein G or Protein A Dynabeads were used for precipitating the antibody-antigen complexes.

Supplementary information for this article is available online: http://emboj.embopress.org

Acknowledgements

We thank Dr Attila Toth for antibodies and for discussion, Dr Alberto Pendas and Dr Christer Höög for antibodies, and Dr Uddipta Biswas and Dr Michelle Stevense for expert help. This study was funded by the German Research Foundation, DFG, through SPP1384 Grant JE150/10-2.

Author contributions

TW and FM designed and performed experiments and edited the manuscript; RJ designed the project and wrote the manuscript. All authors discussed the project at all stages.

Conflict of interest

The authors declare that they have no conflict of interest.

References

Adelfalk C, Janschek J, Revenkova E, Blei C, Liebe B, Gob E, Alsheimer M, Benavente R, de Boer E, Novak I, Hoog C, Scherthan H, Jessberger R (2009) Cohesin SMC1beta protects telomeres in meiocytes. *J Cell Biol* 187: 185–199

Balbas-Martinez C, Sagrera A, Carrillo-de-Santa-Pau E, Earl J, Marquez M, Vazquez M, Lapi E, Castro-Giner F, Beltran S, Bayes M, Carrato A, Cigudosa JC, Dominguez O, Gut M, Herranz J, Juanpere N, Kogevinas M, Langa X, Lopez-Knowles E, Lorente JA *et al* (2013) Recurrent inactivation of STAG2 in bladder cancer is not associated with aneuploidy. *Nat Genet* 45: 1464–1469

Bannister LA, Reinholdt LG, Munroe RJ, Schimenti JC (2004) Positional cloning and characterization of mouse mei8, a disrupted allele of the meiotic cohesin Rec8. *Genesis* 40: 184–194

Bisht KK, Daniloski Z, Smith S (2013) SA1 binds directly to DNA through its unique AT-hook to promote sister chromatid cohesion at telomeres. *J Cell Sci* 126: 3493–3503

Biswas U, Wetzker C, Lange J, Christodoulou E, Seifert M, Beyer A, Jessberger R (2013) Meiotic cohesin SMC1β provides prophase I centromeric cohesion and is required for multiple synapsis-associated functions. *PLoS Genet* 9: e1003985. doi: 10.1371/journal.pgen.1003985

Caburet S, Arboleda VA, Llano E, Overbeek PA, Barbero JL, Oka K, Harrison W, Vaiman D, Ben-Neriah Z, Garcia-Tunon I, Fellous M, Pendas AM, Veitia RA, Vilain E (2014) Mutant cohesin in premature ovarian failure. *N Engl J Med* 370: 943–949

Canudas S, Smith S (2009) Differential regulation of telomere and centromere cohesion by the Scc3 homologues SA1 and SA2, respectively, in human cells. *J Cell Biol* 187: 165–173

Daniel K, Lange J, Hached K, Fu J, Anastassiadis K, Roig I, Cooke HJ, Stewart AF, Wassmann K, Jasin M, Keeney S, Toth A (2011) Meiotic homologue alignment and its quality surveillance are controlled by mouse HORMAD1. *Nat Cell Biol* 13: 599–610

Eijpe M, Heyting C, Gross B, Jessberger R (2000) Association of mammalian SMC1 and SMC3 proteins with meiotic chromosomes and synaptonemal complexes. *J Cell Sci* 113(Pt 4): 673–682

Fukuda T, Daniel K, Wojtasz L, Toth A, Hoog C (2010) A novel mammalian HORMA domain-containing protein, HORMAD1, preferentially associates with unsynapsed meiotic chromosomes. *Exp Cell Res* 316: 158–171

Fukuda T, Pratto F, Schimenti JC, Turner JM, Camerini-Otero RD, Hoog C (2012) Phosphorylation of chromosome core components may serve as axis marks for the status of chromosomal events during mammalian meiosis. *PLoS Genet* 8: e1002485

Fukuda T, Fukuda N, Agostinho A, Hernández-Hernández A, Kouznetsova A, Höög C (2014) STAG3-mediated stabilization of REC8 cohesin

complexes promotes chromosome synapsis during meiosis. *EMBO J* 33: 1243–1255

Garcia-Cruz R, Brieno MA, Roig I, Grossmann M, Velilla E, Pujol A, Cabero L, Pessarrodona A, Barbero JL, Garcia Caldes M (2010) Dynamics of cohesin proteins REC8, STAG3, SMC1{beta} and SMC3 are consistent with a role in sister chromatid cohesion during meiosis in human oocytes. *Hum Reprod* 25: 2316–2327

Gutierrez-Caballero C, Herran Y, Sanchez-Martin M, Suja JA, Barbero JL, Llano E, Pendas AM (2011) Identification and molecular characterization of the mammalian alpha-kleisin RAD21L. *Cell Cycle* 10: 1477–1487

Habu T, Taki T, West A, Nishimune Y, Morita T (1996) The mouse and human homologs of DMC1, the yeast meiosis-specific homologous recombination gene, have a common unique form of exon-skipped transcript in meiosis. *Nucleic Acids Res* 24: 470–477

Haering CH, Jessberger R (2012) Cohesin in determining chromosome architecture. *Exp Cell Res* 318: 1386–1393

Hauf S, Roitinger E, Koch B, Dittrich CM, Mechtler K, Peters JM (2005) Dissociation of cohesin from chromosome arms and loss of arm cohesion during early mitosis depends on phosphorylation of SA2. *PLoS Biol* 3: e69

Herran Y, Gutierrez-Caballero C, Sanchez-Martin M, Hernandez T, Viera A, Barbero JL, de Alava E, de Rooij DG, Suja JA, Llano E, Pendas AM (2011) The cohesin subunit RAD21L functions in meiotic synapsis and exhibits sexual dimorphism in fertility. *EMBO J* 30: 3091–3105

Houmard B, Small C, Yang L, Naluai-Cecchini T, Cheng E, Hassold T, Griswold M (2009) Global gene expression in the human fetal testis and ovary. *Biol Reprod* 81: 438–443

Ishiguro K, Kim J, Fujiyama-Nakamura S, Kato S, Watanabe Y (2011) A new meiosis-specific cohesin complex implicated in the cohesin code for homologous pairing. *EMBO Rep* 12: 267–275

Jessberger R, Podust V, Hubscher U, Berg P (1993) A mammalian protein complex that repairs double-strand breaks and deletions by recombination. *J Biol Chem* 268: 15070–15079

Jessberger R (2010) Deterioration without replenishment–the misery of oocyte cohesin. *Genes Dev* 24: 2587–2591

Jessberger R (2012) Age-related aneuploidy through cohesion exhaustion. *EMBO Rep* 13: 539–546

Lara-Pezzi E, Pezzi N, Prieto I, Barthelemy I, Carreiro C, Martinez A, Maldonado-Rodriguez A, Lopez-Cabrera M, Barbero JL (2004) Evidence of a transcriptional co-activator function of cohesin STAG/SA/Scc3. *J Biol Chem* 279: 6553–6559

Lee J, Hirano T (2011) RAD21L, a novel cohesin subunit implicated in linking homologous chromosomes in mammalian meiosis. *J Cell Biol* 192: 263–276

Liebe B, Alsheimer M, Hoog C, Benavente R, Scherthan H (2004) Telomere attachment, meiotic chromosome condensation, pairing, and bouquet stage duration are modified in spermatocytes lacking axial elements. *Mol Biol Cell* 15: 827–837

Liu L, Keefe DL (2008) Defective cohesin is associated with age-dependent misaligned chromosomes in oocytes. *Reprod Biomed Online* 16: 103–112

Llano E, Herran Y, Garcia-Tunon I, Gutierrez-Caballero C, de Alava E, Barbero JL, Schimenti J, de Rooij DG, Sanchez-Martin M, Pendas AM (2012) Meiotic cohesin complexes are essential for the formation of the axial element in mice. *J Cell Biol* 197: 877–885

Llano E, Gomez HL, Garcia-Tunon I, Sanchez-Martin M, Caburet S, Barbero JL, Schimenti JC, Veitia RA, Pendas AM (2014) STAG3 is a strong candidate gene for male infertility. *Hum Mol Genet*. doi: 10.1093/hmg/ddu051

Losada A, Yokochi T, Kobayashi R, Hirano T (2000) Identification and characterization of SA/Scc3p subunits in the Xenopus and human cohesin complexes. *J Cell Biol* 150: 405–416

Michaelis C, Ciosk R, Nasmyth K (1997) Cohesins: chromosomal proteins that prevent premature separation of sister chromatids. *Cell* 91: 35–45

Nasmyth K, Haering CH (2009) Cohesin: its roles and mechanisms. *Annu Rev Genet* 43: 525–558

Nasmyth K (2011) Cohesin: a catenase with separate entry and exit gates? *Nat Cell Biol* 13: 1170–1177

Nogues C, Fernandez C, Rajmil O, Templado C (2009) Baseline expression profile of meiotic-specific genes in healthy fertile males. *Fertil Steril* 92: 578–582

Onn I, Heidinger-Pauli JM, Guacci V, Unal E, Koshland DE (2008) Sister chromatid cohesion: a simple concept with a complex reality. *Annu Rev Cell Dev Biol* 24: 105–129

Page J, Viera A, Parra MT, de la Fuente R, Suja JA, Prieto I, Barbero JL, Rufas JS, Berrios S, Fernandez-Donoso R (2006) Involvement of synaptonemal complex proteins in sex chromosome segregation during marsupial male meiosis. *PLoS Genet* 2: e136

Pezzi N, Prieto I, Kremer L, Perez Jurado LA, Valero C, Del Mazo J, Martinez AC, Barbero JL (2000) STAG3, a novel gene encoding a protein involved in meiotic chromosome pairing and location of STAG3-related genes flanking the Williams-Beuren syndrome deletion. *FASEB J* 14: 581–592

Pittman DL, Cobb J, Schimenti KJ, Wilson LA, Cooper DM, Brignull E, Handel MA, Schimenti JC (1998) Meiotic prophase arrest with failure of chromosome synapsis in mice deficient for Dmc1, a germline-specific RecA homolog. *Mol Cell* 1: 697–705

Prieto I, Suja JA, Pezzi N, Kremer L, Martinez AC, Rufas JS, Barbero JL (2001) Mammalian STAG3 is a cohesin specific to sister chromatid arms in meiosis I. *Nat Cell Biol* 3: 761–766

Prieto I, Pezzi N, Buesa JM, Kremer L, Barthelemy I, Carreiro C, Roncal F, Martinez A, Gomez L, Fernandez R, Martinez AC, Barbero JL (2002) STAG2 and Rad21 mammalian mitotic cohesins are implicated in meiosis. *EMBO Rep* 3: 543–550

Prieto I, Tease C, Pezzi N, Buesa JM, Ortega S, Kremer L, Martinez A, Martinez AC, Hulten MA, Barbero JL (2004) Cohesin component dynamics during meiotic prophase I in mammalian oocytes. *Chromosome Res* 12: 197–213

Remeseiro S, Cuadrado A, Carretero M, Martinez P, Drosopoulos WC, Canamero M, Schildkraut CL, Blasco MA, Losada A (2012a) Cohesin-SA1 deficiency drives aneuploidy and tumourigenesis in mice due to impaired replication of telomeres. *EMBO J* 31: 2076–2089

Remeseiro S, Cuadrado A, Gomez-Lopez G, Pisano DG, Losada A (2012b) A unique role of cohesin-SA1 in gene regulation and development. *EMBO J* 31: 2090–2102

Revenkova E, Eijpe M, Heyting C, Hodges CA, Hunt PA, Liebe B, Scherthan H, Jessberger R (2004) Cohesin SMC1 beta is required for meiotic chromosome dynamics, sister chromatid cohesion and DNA recombination. *Nat Cell Biol* 6: 555–562

Scherthan H (2001) A bouquet makes ends meet. *Nat Rev Mol Cell Biol* 2: 621–627

Shintomi K, Hirano T (2010) Sister chromatid resolution: a cohesin releasing network and beyond. *Chromosoma* 119: 459–467

Siderakis M, Tarsounas M (2007) Telomere regulation and function during meiosis. *Chromosome Res* 15: 667

Solomon DA, Kim T, Diaz-Martinez LA, Fair J, Elkahloun AG, Harris BT, Toretsky JA, Rosenberg SA, Shukla N, Ladanyi M, Samuels Y, James CD, Yu H, Kim JS, Waldman T (2011) Mutational inactivation of STAG2 causes aneuploidy in human cancer. *Science* 333: 1039–1043

Sumara I, Vorlaufer E, Gieffers C, Peters BH, Peters JM (2000) Characterization of vertebrate cohesin complexes and their regulation in prophase. *J Cell Biol* 151: 749 – 762

Wojtasz L, Daniel K, Roig I, Bolcun-Filas E, Xu H, Boonsanay V, Eckmann CR, Cooke HJ, Jasin M, Keeney S, McKay MJ, Toth A (2009) Mouse HORMAD1 and HORMAD2, two conserved meiotic chromosomal proteins, are depleted from synapsed chromosome axes with the help of TRIP13 AAA-ATPase. *PLoS Genet* 5: e1000702

Wood AJ, Severson AF, Meyer BJ (2010) Condensin and cohesin complexity: the expanding repertoire of functions. *Nat Rev Genet* 11: 391 – 404

Xiao T, Wallace J, Felsenfeld G (2011) Specific sites in the C terminus of CTCF interact with the SA2 subunit of the cohesin complex and are required for cohesin-dependent insulation activity. *Mol Cell Biol* 31: 2174 – 2183

Xu H, Beasley MD, Warren WD, van der Horst GT, McKay MJ (2005) Absence of mouse REC8 cohesin promotes synapsis of sister chromatids in meiosis. *Dev Cell* 8: 949 – 961

Yoshida K, Kondoh G, Matsuda Y, Habu T, Nishimune Y, Morita T (1998) The mouse RecA-like gene Dmc1 is required for homologous chromosome synapsis during meiosis. *Mol Cell* 1: 707 – 718

Yuan L, Brundell E, Hoog C (1996) Expression of the meiosis-specific synaptonemal complex protein 1 in a heterologous system results in the formation of large protein structures. *Exp Cell Res* 229: 272 – 275

